Orientation Development in the Tubular Film Extrusion of Polypropylene

YASUSHI SHIMOMURA,* JOSEPH E. SPRUIELL, and JAMES L. WHITE, *Polymer Engineering, Universitiy of Tennessee, Knoxville, Tennessee 37916*

Synopsis

A basic study of orientation development in the tubular film extrusion of polypropylene is reported. WAXS and birefringence measurements were carried out on films prepared under conditions of known blowup ratio B, drawdown v_L/v_0, machine direction tension, and bubble pressure. Pole figures were constructed and biaxial orientation factors determined. The use of an orientation factor triangle diagram was found to be a useful method of representing the variation of orientation with processing conditions. The variation in orientation with processing parameters for polypropylene was found to have similar behavior to that previously found for polyethylene.

INTRODUCTION

Tubular film extrusion is one of the most important of polymer processing operations as it represents the major method of manufacture of film. No aspect of the study of tubular film extrusion is more important than the relationship of the structure, including orientation and crystalline morphology, to the processing conditions. While there have now been a number of studies of the structure of tubular film,[1–16] these are almost entirely limited to polyethylene. Few of these relate their observations to the specific processing conditions. This deficiency has in part been overcome by the recent studies of Maddams and Preedy[5–8] and of Choi and the present authors,[9,10] who have investigated polyethylene[5–8,10] and polystyrene.[9] There have been no reported studies of tubular film produced from polypropylene.

It is our purpose in the present paper to make a basic study of the development of the structure of polypropylene tubular film. We seek to relate the characteristics of the film to the processing conditions. This paper presents both an extension of our earlier studies of structure development in tubular film extrusion[9,10] and of the melt processing of polypropylene.[11–13]

KINEMATICS AND DYNAMICS OF TUBULAR FILM EXTRUSION

It is useful to concisely summarize the kinematics and force balances applicable to tubular film extrusion. These have been developed in a series of papers by Pearson and Petrie.[14–16] If we take 1 as the machine direction, 2 as the transverse direction, and 3 the thickness direction, we may write the velocity gradients in a tubular film process (see Figure 1) as

$$\frac{\partial v_1}{\partial \xi_1} = \frac{Q \cos\theta}{2\pi Rh}\left(-\frac{1}{h}\frac{dh}{dz} - \frac{1}{R}\frac{dR}{dz}\right) \tag{1a}$$

* Permanent address: Ube Industries, Hirakata Plastics Laboratory, Hirakata, Osaka, Japan

Journal of Applied Polymer Science, Vol. 27, 2663–2674 (1982)

CCC 0021-8995/82/072663-12$02.20

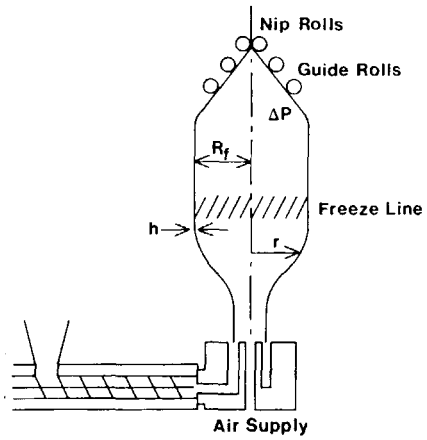

Fig. 1. Tubular film process.

$$\frac{\partial v_2}{\partial \xi_2} = \frac{Q \cos\theta}{2\pi Rh}\left(\frac{1}{R}\frac{dR}{dz}\right) \tag{1b}$$

$$\frac{\partial v_3}{\partial \xi_3} = \frac{Q \cos\theta}{2\pi Rh}\left(\frac{1}{h}\frac{dh}{dz}\right) \tag{1c}$$

Here Q is the extrusion rate, h is the film thickness, and θ is the angle between the axis of the bubble and the tangent to the surface of the bubble, and R is the bubble radius at any height z above the extruder exit.

Different special kinematic cases may be cited. For uniaxial extension

$$\frac{\partial v_2}{\partial \xi_2} = \frac{\partial v_3}{\partial \xi_3}, \qquad \frac{1}{R}\frac{dR}{dz} = \frac{1}{h}\frac{dh}{dz} \tag{2a}$$

When uniaxial extension exists uniformly throughout the bubble this leads to

$$\frac{v_L}{v_0} = \left(\frac{R_0}{R_L}\right)^2 = \frac{1}{B^2} \tag{2b}$$

where R_0 is the initial bubble radius and R_L the final bubble radius, v_0 and v_L, the initial and final film velocities. B is the blowup ratio. For planar extension

$$\frac{\partial v_2}{\partial \xi_2} = 0, \qquad \frac{1}{R}\frac{dR}{dz} = 0 \tag{3a}$$

which leads to

$$B = 1 \tag{3b}$$

For equal biaxial extension

$$\frac{\partial v_1}{\partial \xi_1} = \frac{\partial v_2}{\partial \xi_2}, \qquad -\frac{1}{R}\frac{dR}{dz} - \frac{1}{h}\frac{dh}{dz} = \frac{1}{R}\frac{dR}{dz} \tag{4a}$$

When this occurs uniformly,

$$v_L/v_0 = B \tag{4b}$$

The force balance on the film may be shown to have the form[14–16]

$$F_L = 2\pi Rh\sigma_{11}\cos\theta + \pi\Delta p(R_L{}^2 - R^2) \tag{5a}$$

$$\Delta p = \frac{h\sigma_{11}}{R_1} + \frac{h\sigma_{22}}{R_2} \tag{5b}$$

where F_L is the takeup tension, Δp the inflation pressure, σ_{11} and σ_{22} the stresses in the machine and transverse direction, and R_1 and R_2 the principal radii of curvature of the film.

EXPERIMENTAL

Materials

A Hercules Profax PD 195 with a melt index of 1.5 was used in this study. The shear viscosity η and principal normal stress difference N_1 were determined for this melt at 190°C in a Rheometrics Mechanical Spectrometer using the cone-plate mode.[17,18] This is shown in Figure 2 as a function of shear stress. Using Minoshima et al.'s[19] correlation of rheological properties and molecular weight distribution, these data indicate a moderately narrow molecular weight distribution ($M_w/M_n \sim 3.0$–5.0)

Preparation of Films

The tubular film was produced with a 0.75-in. Rainville screw extruder with an annular blown film die (inside diameter of 1.496 cm and an outside diameter of 1.605 cm). The extrusion temperature was 210°C.

A series of seven films were produced under the conditions listed in Table I. We attempted to produce three classes of films. One group was formed under

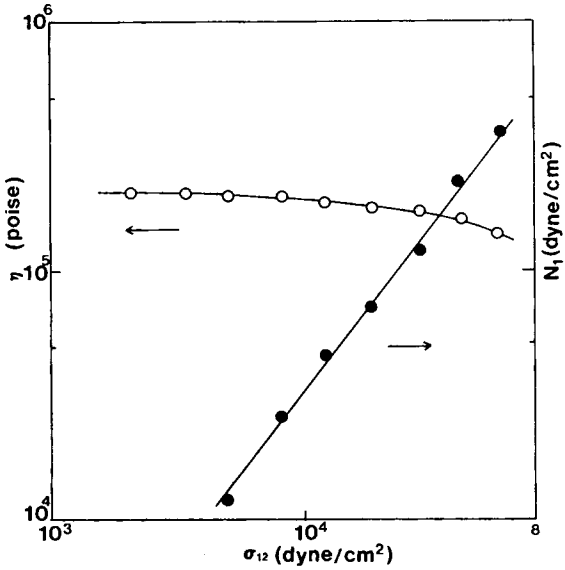

Fig. 2. Viscosity η and principal normal stress difference N_1 vs. shear stress of polypropylene melt studied at 190°C.

TABLE I
Summary of Polypropylene Films Prepared

Film Designation	Blowup ratio B	Drawdown ratio v_L/v_0	Film thickness (μm)	Stresses (MPa) σ_{11}	σ_{22}
Uniaxial					
P110	0.36	3.0	360	0.194 ± 0.032	0
P114	0.24	8.0	206	0.556 ± 0.045	0
P118	0.16	17.6	140	0.878 ± 0.202	0
Constant blowup ratio					
P106	1.0	8.0	39	0.574 ± 0.02	0.074 ± 0.005
P119	1.0	17.6	22	0.876 ± 0.05	0.128 ± 0.01
P103	1.4	3.0	97	0.216 ± 0.028	0.056 ± 0.002
P107	1.4	8.0	28	0.55 ± 0.017	0.143 ± 0.006
P120	1.4	17.6	16	0.829 ± 0.085	0.249 ± 0.010
Equal biaxial					
P104	3.0	3.0	46	0.302 ± 0.030	0.205 ± 0.008

uniaxial extension, and a second group was produced with constant blowup ratio while one sample was produced with $v_L/v_0 = B$, the kinematic condition for equal biaxial extension. The pressures inside of the bubble were measured with a manometer, and the longitudinal tensions in the tubular film during processing were measured with a Tensitron Web Tension Sensor.

Wide Angle X-Ray Scattering (WAXS)

Pole figures[20] showing the distribution of the normals (poles) of the (110) and (040) planes of crystalline polypropylene were prepared using a single crystal orienter mounted on a General Electric XRD-5 Diffractometer. The technique was essentially that of Heffelfinger and Burton[21] and was the same as was used in our earlier study of crystalline orientation of polyethylene tubular film.[10] The technique is described in more detail there.

The radiation used was CuKα with a wavelength of 1.542 Å. Films prepared in the tubular film process were stacked and glued at their edges and mounted on the single crystal orienter. The diffractometer was set at a fixed diffraction angle, 2θ, for diffraction from either the (110) or (040) planes, and the sample was rotated and tilted by the single crystal orienter in order to determine the intensity distribution needed for pole figure plotting and computation of $\overline{\cos^2\phi}$ values needed in the evaluation of orientation factors.

Because of the inherent biaxial nature of orientation in polymer films, the intensity data were used to compute biaxial orientation factors defined after White and Spruiell.[9,10,22,23] These factors are given by

$$f_{1j}^B = 2\,\overline{\cos^2\phi_{j1}} + \overline{\cos^2\phi_{j2}} - 1$$
$$f_{2j}^B = 2\,\overline{\cos^2\phi_{j2}} + \overline{\cos^2\phi_{j1}} - 1 \qquad (6)$$

where j represents a crystallographic axis (normally a, b, or c) and $\overline{\cos^2\phi_{jk}}$ is the average value of the square of the cosine of the angle between the j crystallographic axis and reference direction k ($k = 1$ for machine direction, $k = 2$ for transverse or circumferential direction in the film). In the event that uniaxial orientation relative to the machine direction exists, the f_{1j}^B reduce to the well-known Hermans–Stein orientation factors and the f_{2j}^B are zero.

WAXS patterns of the polypropylene films indicated that they had the monoclinic structure of Natta and Corradini[24] similar to that observed in melt spun fibers.[11,12] Thus the b-axis orientation factors could be computed directly from the 040 intensity distribution, since the (040) planes are perpendicular to the b-axis in monoclinic polypropylene. The polypropylene chain has a helical conformation with the axis of the helix parallel to the c-axis of the unit cell. There is no set of reflecting planes which are perpendicular to the c-axis. Wilchinsky[25,26] has derived equations relating the variation of the intensity distribution in the 110 and 040 reflections to the $\overline{\cos^2\phi_{ck}}$ values, and we have used these relationships in the computation of the c-axis orientation factors. We also computed the orientation of an a'-axis, which is defined as perpendicular to the plane of the b and c axes. The angle between the a and a' axes is small (less than 10°).

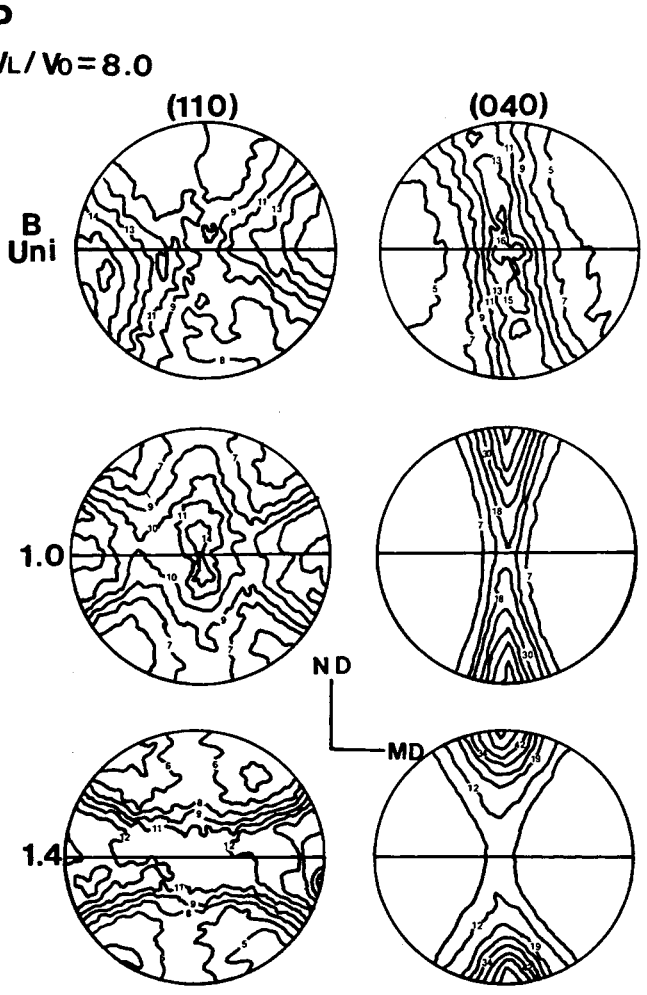

Fig. 3. Pole figures for the 110 and 040 reflections at a drawdown ratio of 8.0. Units on the contours are 10 times the intensity for a random sample.

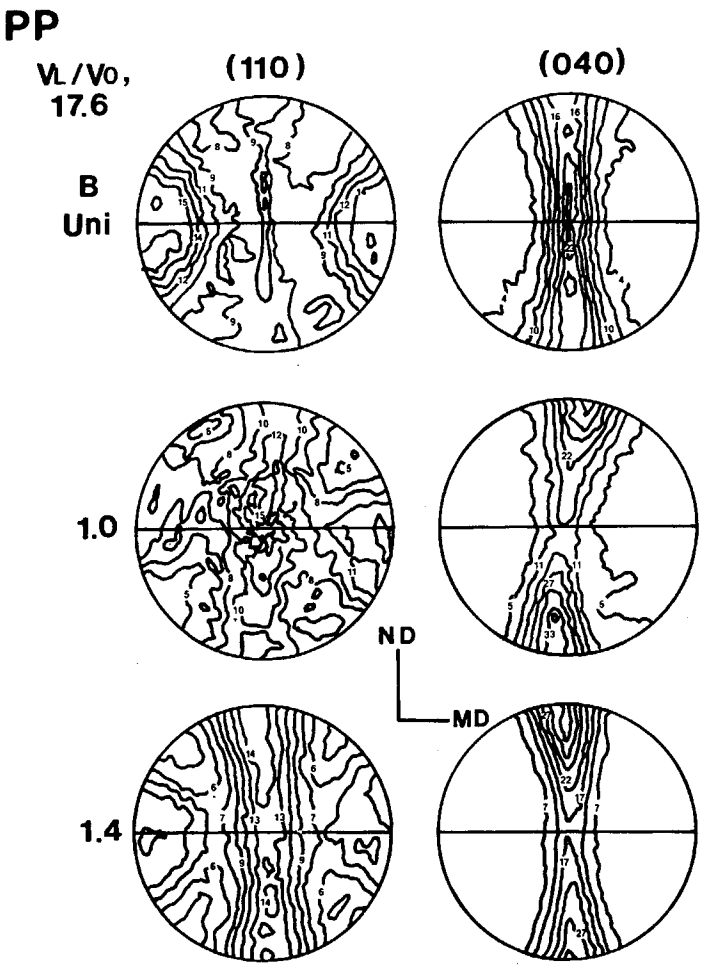

Fig. 4. Pole figures for the 110 and 040 reflections at a drawdown ratio at 17.6.

Birefringence

Birefringence measurements were made using a Babinet compensator and an experimental arrangement equivalent to that developed by Stein,[27] which allows a sample to be rotated and tilted in the incident light beam. This instrument provides for measurement of all three birefringences of biaxially oriented films and was used in our previous studies of orientation in polystyrene[9,22] and polyethylene[10] film.

RESULTS

Pole figures for the 110 and 040 reflections are shown for a series of four films in Figures 3–6. Figures 3 and 4 present the results for the case of constant drawdown ratio at 8.0 and 17.6, respectively. For the approximately uniaxial case, the (040) poles, i.e., the *b*-axes are approximately perpendicular to the machine direction and distributed almost uniformly about it. There is a very slight tendency for (040) poles to concentrate near the transverse direction. With increasing blowup ratio, the *b*-axes become concentrated in the normal direction.

Figure 5 presents the results for the case of a constant blowup ratio of 1.4. The b-axis distributions show concentration in the normal direction. With increasing drawdown ratio, the b-axes show an increasing tendency toward symmetry about the machine direction. Figure 6 presents the results for the case of drawdown of 3.0 and blowup ratio of 3.0, which corresponds to the kinematic condition for equal biaxial orientation. The b-axes concentrate in the normal direction.

Generally, the (110) pole figures are quite complicated. For the uniaxial case, the (110) poles concentrate in a band making an angle of about 50–60° to the machine direction. On the other hand, for the biaxial case, the (110) poles are distributed around the normal direction in the *MD–TD* plane (~90° to *ND*) with a slight tendency to concentrate in the transverse direction.

Biaxial orientation factors were determined for the seven films as summarized in Table II. They are shown plotted in an orientation function triangle diagram in Figure 7. The machine direction orientation factors, f_1^B, are also plotted vs. the drawdown ratio in Figure 8 for the uniaxial and constant blowup ratio films.

For the uniaxial films all of the f_2^B values ($f_{c2}^B, f_{b2}^B, f_{a2}^B$) are near zero as expected. The f_{c1}^B values are positive and increase with drawdown ratio, while the f_{b1}^B values are negative and decrease with drawdown ratio. The f_{a1}^B are near zero but slightly positive throughout the range of conditions investigated.

The films with constant blowup ratio of 1.4 generally have f_2^B values which differ substantially from zero (Fig. 7). The f_{c1}^B values increase and the f_{b1}^B values decrease with drawdown ratio in a manner similar to that for the uniaxial films [Fig. 8(b)], but these orientation factors are greater in absolute magnitude at a given drawdown than for the uniaxial samples. The f_{a1}^B values go through a maximum positive value and then become negative at high drawdown ratios. The f_{c2}^B and f_{b2}^B values decrease in absolute magnitude with increasing drawdown ratio, indicating a tendency toward more nearly uniaxial orientation with respect to the machine direction at high drawdown ratios.

The orientation factors for the sample produced with $v_L/v_0 = B = 3.0$ are also shown plotted in Figure 7. The results lie very near to the dashed line at 45° to the f_1^B and f_2^B axes, indicating that the kinematic condition does give orientation that is close to equal biaxial.

Birefringence data on the films are shown in Table II and plotted in Figure 9 as a function of drawdown ratio. For the approximately uniaxial case, the values of Δn_{13} and Δn_{12} are positive, have almost the same value, and increase with drawdown ratio. The values of Δn_{23} are almost zero.

TABLE II
Characteristics of Polypropylene Films

Film designation	WAXS orientation factor						Birefringence × 10^3		
	b axis		c axis		a axis				
	f_{1b}^B	f_{2b}^B	f_{1c}^B	f_{2c}^B	f_{1a}^B	f_{2a}^B	Δn_{13}	Δn_{23}	Δn_{12}
P110	−0.228	−0.061	0.174	0.080	0.053	−0.019	5.29	1.13	4.16
P114	−0.287	−0.058	0.195	0.078	0.091	−0.020	6.90	0.543	6.26
P118	−0.337	−0.035	0.272	0.076	0.066	−0.040	8.16	−0.20	8.36
P103	−0.435	−0.286	0.298	0.222	0.137	0.064	5.73	3.26	2.47
P107	−0.455	−0.281	0.324	0.170	0.131	0.110	9.05	3.64	5.41
P120	−0.397	−0.161	0.489	0.165	−0.092	−0.003	11.77	3.45	8.32
P104	−0.394	−0.336	0.261	0.174	0.133	0.162	5.71	4.97	0.742

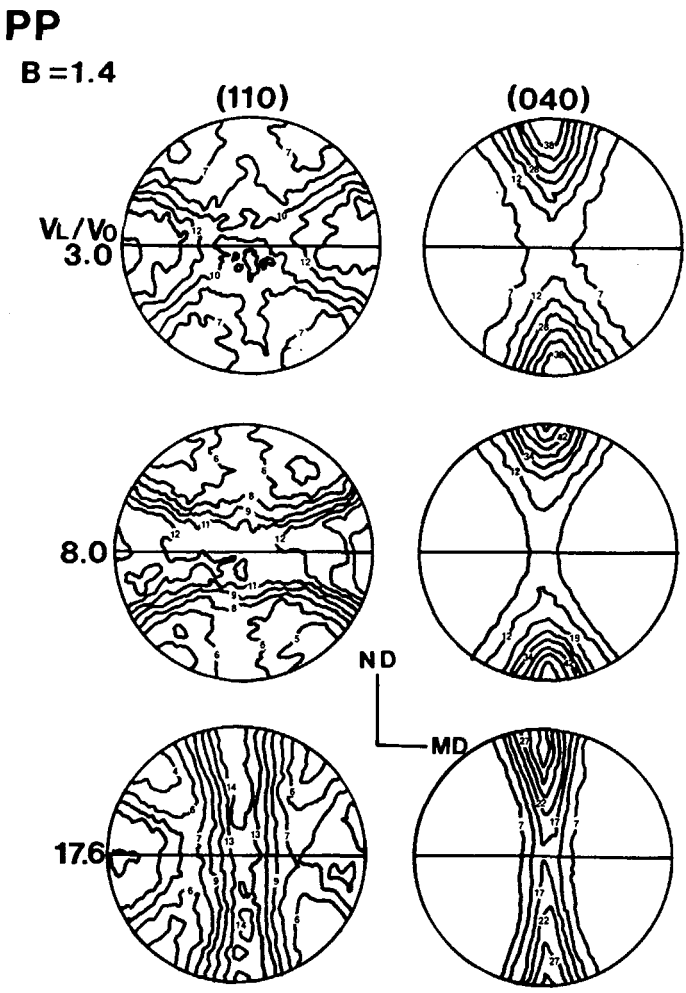

Fig. 5. Pole figures of the 110 and 040 reflections at a blowup ratio of 1.4.

For the constant blowup ratio series ($B = 1.4$) the values of Δn_{13}, Δn_{12}, and Δn_{23} are positive; and the values of Δn_{13} are larger than those of Δn_{12} and Δn_{23}. The values of Δn_{13} and Δn_{12} increase with drawdown ratio.

In Figure 10 a plot birefringence values as a function of blowup ratio is shown for a constant drawdown ratio of 3.0. As blowup ratio increases the value of Δn_{23} increases and approaches the value of Δn_{13} at blowup ratio equal 3.0, while Δn_{12} decreases to a value near zero.

DISCUSSION

It is first of interest to contrast the crystalline orientation of the polypropylene films with that observed by earlier investigators for polyethylene.

The pole figures for the (040) poles are similar in appearance to (020) pole figures of polyethylene and the f_{1b}^{B} orientation factors of polypropylene tubular films have almost the same trends as for polyethylene tubular films.[10] In both cases the values of f_{b1}^{B} become increasingly negative with increasing drawdown

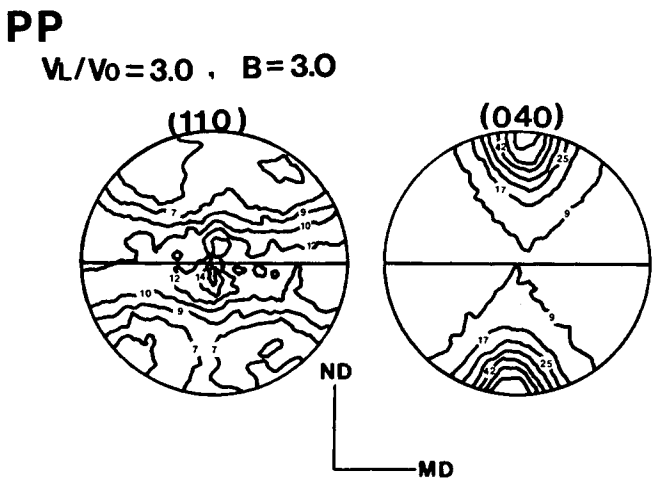

Fig. 6. Pole figures for the 110 and 040 reflections at a drawdown ratio of 3.0, blowup ratio 3.0.

ratio until the b-axes are essentially perpendicular to the machine direction. As blowup increases at a given drawdown, there is a tendency for the b-axes to becomes increasingly concentrated in the normal direction, i.e., perpendicular to the surface of the film. The c-axis orientation factors of polypropylene films also have similar behavior to those of polyethylene films. With increasing

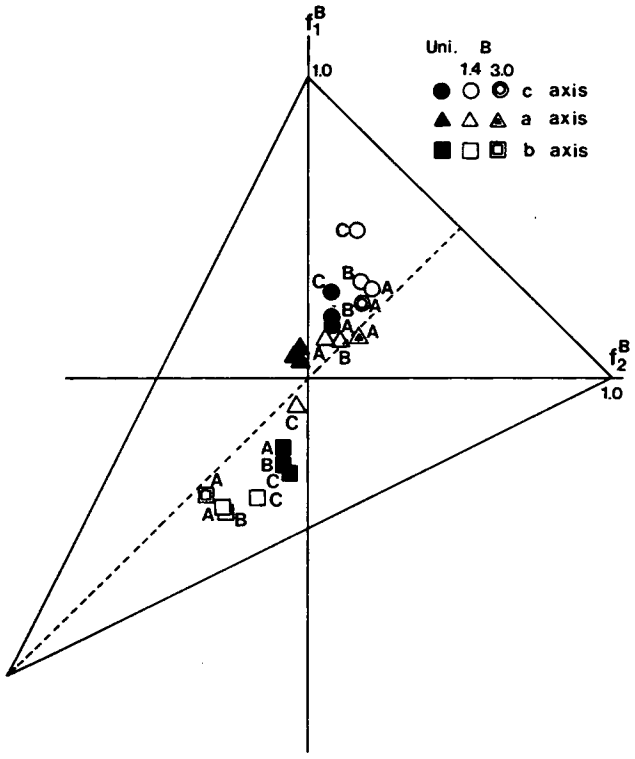

Fig. 7. Orientation function triangle diagram for polypropylene blown film; v_L/v_0: (A) 3.0; (B) 8.0; (C) 17.6.

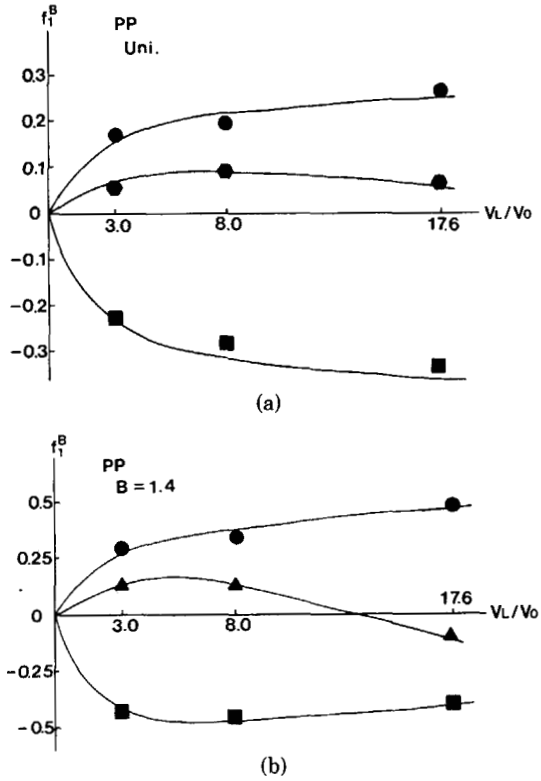

Fig. 8. Variation of orientation factors f_1^B with *D*rawdown *R*atio v_L/v_0: (a) uniaxial films; (b) blowup ratio = 1.4. (●) *c*-axis; (●) *a*-axis; (■) *b*-axis.

drawdown ratio, there is greater chain alignment in the machine direction in the film. The f_{c1}^B values rise more rapidly with drawdown ratio for the constant blowup ratio series than for the uniaxial series. Increasing blowup tends to produce a shift of chain alignment toward the transverse direction of the film in both cases.[10] These results suggest that the crystalline morphology of these polypropylene films is similar to that for polyethylene films described in more detail in our earlier paper.[10]

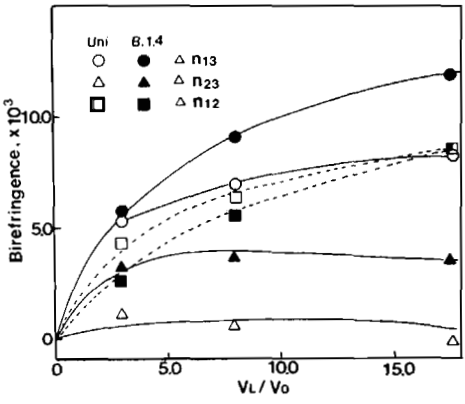

Fig. 9. Variation of birefringence with drawdown ratio v_L/v_0.

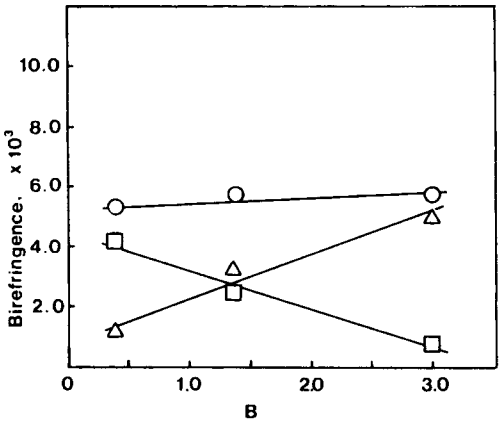

Fig. 10. Variation of birefringence with blowup ratio at a contant drawdown ratio of 3.0: (□) Δn_{12}; (○) Δn_{13}; (△) Δn_{23}.

We have attempted to correlate the orientation developed in these polypropylene films with the measured stresses at crystallization in a manner similar to that of Choi et al. for the case of polystyrene[9] and polyethylene.[10] The longitudinal and hoop stresses in the bubble at crystallization are determined from the measured tension and inflation pressure through [compare eq. (5)]

$$\sigma_{11} = F_L/2\pi Rh, \qquad \sigma_{22} = \Delta pR/h \tag{7a,b}$$

The stresses computed in this manner for the polypropylene films are presented in Table I. It should be noted that, due to the small magnitude of the forces involved and other experimental difficulties in making such measurements for polypropylene, the errors in these stress values are relatively large in the present case. Thus care must be exercised in their interpretation.

Qualitatively, the trends of the orientation vs. stress behavior are similar to those observed for polyethylene film by Choi et al.[10] For example, there is a reasonably satisfactory correlation between birefringence, Δn_{ij}, and principal stress difference $\sigma_i - \sigma_j$, as shown in Figure 11. Nadella et al.[12] have correlated the birefringence of melt spun polypropylene fibers with spinline stress. We show a band representing their data in the range of stresses measured for our films in Figure 11. Considering the numerous sources of error, especially an

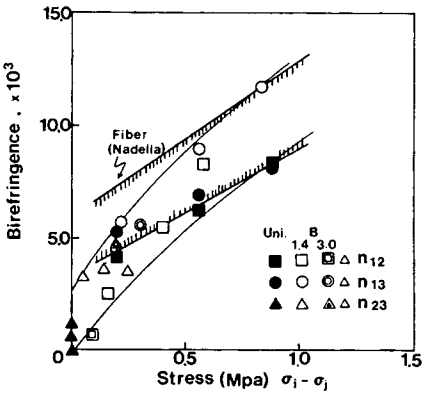

Fig. 11. Variation of birefringence with the difference in principal stresses.

inadequate correction for gravitational forces at low stress values in the fiber data, the agreement is satisfactory. Choi, Spruiell, and White[10] have suggested that such correlations are due to the fact that the orientation and morphology of semicrystalline polymers should be functionally related to the state of orientation existing in the melt just prior to crystallization. This melt orientation is related to the stress state through the rheo-optical law

$$\Delta n_{ij} = C(\sigma_i - \sigma_j) \tag{8}$$

where C is the stress optical coefficient. It is important to note that eq. (8) does not relate the birefringence of the final solidified film or fiber to the applied stress state. For semicrystalline polymers there is a large increase in orientation during crystallization due to oriented nucleation and growth processes.

The present stress data do not appear to be sufficiently accurate enough to warrant more detailed analysis of the orientation-stress relationship.

This research was supported by the National Science Foundation through NSF Grant Eng 78-21889.

References

1. D. R. Holmes and R. P. Palmer, *J. Polym. Sci.*, **31**, 345 (1958).
2. P. H. Lindenmeyer and S. Lustig, *J. Appl. Polym. Sci.*, **9**, 227 (1963).
3. C. R. Desper, *J. Appl. Polym. Sci.*, **13**, 169 (1969).
4. T. Nagasawa, T. Matsumura, S. Hoshino, and K. Kobayoshi, *Appl. Polym. Symp.*, **20**, 275 (1973).
5. W. F. Maddams and J. E. Preedy, *J. Appl. Polym. Sci.*, **22**, 2721 (1978).
6. W. F. Maddams and J. E. Preedy, *J. Appl. Polym. Sci.*, **22**, 2739 (1978).
7. W. F. Maddams and J. E. Preedy, *J. Appl. Polym. Sci.*, **22**, 2751 (1978).
8. W. F. Maddams and J. E. Preedy, *J. Appl. Polym. Sci.*, **22**, 3027 (1978).
9. K. Choi, J. L. White, and J. E. Spruiell, *J. Appl. Polym. Sci.*, **25**, 2777 (1980).
10. K. Choi, J. E. Spruiell, and J. L. White, *J. Polym. Sci., Polym. Phys.* **20**, 27 (1982).
11. J. E. Spruiell and J. L. White, *Polym. Eng. Sci.*, **15**, 660 (1975).
12. H. P. Nadella, H. M. Henson, J. E. Spruiell, and J. L. White, *J. Appl. Polym. Sci.*, **21**, 3003 (1977).
13. W. Minoshima, J. L. White, and J. E. Spruiell, *J. Appl. Polym. Sci.*, **25**, 287 (1980).
14. J. R. A. Pearson and C. J. S. Petrie, *J. Fluid Mech.*, **40**, 1 (1970).
15. J. R. A. Pearson and C. J. S. Petrie, *J. Fluid Mech.*, **42**, 609 (1970).
16. J. R. A. Pearson and C. J. S. Petrie, *Plast. Polym.*, **38**, 85 (1970).
17. K. Walters, *Rheometry*, Chapman and Hall, London, 1975.
18. J. L. White, *Molten Polymers Rheometry: Industrial Applications*, K. Walters, Ed., Wiley, New York, 1980.
19. W. Minoshima, J. L. White, and J. E. Spruiell, *Polym. Eng. Sci.*, **20**, 1166 (1980).
20. L. E. Alexander, *X-ray Diffraction Methods in Polymer Science*, Wiley, New York, 1969.
21. C. J. Heffelfinger and R. L. Burton, *J. Polym. Sci.*, **47**, 289 (1960).
22. J. L. White and J. E. Spruiell, *Polym. Eng. Sci.*, **21**, 859 (1981).
23. K. Matsumoto, J. F. Fellers, and J. L. White, *J. Appl. Polym. Sci.*, **26**, 85 (1981).
24. G. Natta and P. Corradini, *Nuovo Cimento Suppl.*, **15**, 40 (1960).
25. Z. W. Wilchinsky, *J. Appl. Phys.*, **30**, 792 (1959).
26. Z. W. Wilchinsky, *J. Appl. Phys.*, **31**, 1969 (1960).
27. R. S. Stein, *J. Polym. Sci.*, **24**, 383 (1957).

Received November 2, 1981
Accepted January 28, 1982